SLOPE STABILITY AND SAFETY DISTANCE FOR MINE WASTE ROCK PILES BUILT BY END/PUSH DUMPING

Kasra Majdanishabestari, Gilbert Girumugisha, Carlos Ovalle, Michel Aubertin
Department of Civil, Geological and Mining Engineering,
Polytechnique Montréal
Research Institute of Mining and Environment (RIME) UQAT-Polytechnique,
Québec, Canada

Esteban Sáez
Department of Structural and Geotechnical Engineering
Pontificia Universidad Católica de Chile, Santiago, Chile

ABSTRACT
Large volumes of waste rock (WR) are commonly extracted from open-pit mines and stored in high waste rock piles (WRP), which are generally constructed by end and push dumping with a side slope of around 37°. The safety distance to operate machinery near the edge of a WRP slope can, in principle, be estimated from stability analyses performed with the limit equilibrium method (LEM). However, the corresponding critical slip surface in a large WRP tends to develop in a zone (rather than at a specific location) where the factor of safety (FS) is more or less the same, leading to significant uncertainty. Alternatively, more comprehensive analyses can be conducted by considering the global stress and deformation fields in the WRP and the effects of the construction sequence (i.e., stress history) on its mechanical response. The main objective of this study is to analyze the geotechnical behavior of high WRPs built by end/push-dumping methods in an open-pit mine and to evaluate how the safety distance to the edge of the pile can be established. WR material properties from a hard rock mine were characterized through triaxial tests on 300 mm diameter specimens of relatively coarse material ($d_{max} = 50$ mm). The experimental results show that the behavior of the loose waste rock is contractive and cohesionless, with a shear strength controlled by a state-dependent internal friction angle that can reach up to 45°. The parameters of the Hardening Soil (HS) constitutive model have been calibrated using the experimental results, and finite element simulations were performed with this model for different in pit disposal scenarios. The results indicate that the position of the machinery on the pile surface has a limited effect on the calculated value of FS, but it may significantly affect the location of the sliding surface.
Keywords: mine waste rock piles, large scale laboratory testing, numerical modeling, slope stability analysis.

RÉSUMÉ
De grands volumes de roches stériles sont extraits des mines à ciel ouvert et stockés dans des haldes à stériles de grande dimension, qui sont généralement construites par déversement à la benne ou par poussée au butoir, ce qui produit une pente latéral' d'environ 37°. La distance de sécurité pour opérer la machinerie près du bord de la pente de la halde peut, en principe, être estimée à partir d'analyses de stabilité effectuées avec la méthode d'équilibre limite. Cependant, la surface de glissement critique pour les haldes de grande dimension tend à se développer, dans une zone (plutôt qu'à un emplacement spécifique) où le facteur de sécurité (FS) varie peu, ce qui induit une grande incertitude. Alternativement, des analyses plus élaborées peuvent être menées en considérant le champ des contraintes et des déformations dans la halde et les effets de la séquence de construction (i.e. historique des contraintes) sur sa réponse mécanique. L'objectif principal de cette étude est d'analyser le comportement géotechnique des haldes à stériles construites dans une fosse par déversement et poussée et d'évaluer comment la distance de sécurité au bord de la halde peut être établie. Les propriétés des stériles d'une mine de roche dure ont été caractérisées par des essais triaxiaux sur des éprouvettes de 300 mm de diamètre de matériau relativement grossier ($d_{max} = 50$ mm). Les résultats expérimentaux montrent que le comportement de la roche stérile lâche est contractant et pulvérulent, avec une résistance au cisaillement contrôlée par un angle de frottement interne variant avec l'état de chargement, pouvant atteindre jusqu'à 45°. Les paramètres du modèle constitutif Hardening Soil (HS) ont été calibrés à l'aide des résultats expérimentaux, et des simulations par éléments finis ont été menées avec ce modèle pour différents scénarios de remblayage d'une fosse minière. Les résultats montrent que la position de la machinerie sur la surface de la halde a un effet limité sur la valeur calculée de FS, mais qu'elle peut affecter de manière significative l'emplacement de la surface de glissement.
Mots clés: haldes à stériles, essais de laboratoire, modélisation numérique, stabilité des pentes.

1 INTRODUCTION

Large volumes of mine waste rock (WR) are produced during operations of ore extraction and stored on the surface in waste rock piles (WRP). Piles built with WR material from hard rock mines can reach hundreds of meters in height, with a side slope of around 37° (Aubertin et al., 2002, 2021; Maknoon et Aubertin, 2021). In high

mountainous areas, the valley-fill construction method is typically adopted. It consists in dumping the material down the slope to the valley, with an inclination above its angle of repose (i.e., push- or end-dumping). This technique is used for instance at the Andina mine in Chile (Valenzuela et al., 2008), Antamina mine in Peru (Hawley and Cunning, 2017), and at coal mines in British Columbia (Dawson et al., 1999). End/push-dumping of WR can also be used for open-pit backfilling, as an alternative to the more expensive backfilling from the bottom of the pit (Ouellet et al., 2021).

A safe way to operate with the end/push-dumping method consists in depositing the WR material on the surface using trucks at a predefined safety distance from the edge of the pile, given by the zone of potential sliding surfaces ensuring at least a critical factor of safety (FS_{cr}) (see Figure 1). Then, the material can be pushed by remote-controlled dozers on the surface to the edge, through a waste dump corridor, to avoid compromising the safety of truck's drivers (Bar et al., 2020). The safety distance can be assessed through slope stability analysis. However, simple methods, such as limit equilibrium, can result in a large variability of the critical zone within a narrow range of values around the FS_{cr}, forcing engineers to adopt conservative criteria. On the other hand, a more comprehensive stability analysis, based on the simulated stress and deformation fields of the WRP and the effects of the construction sequence on its response could give more realistic results.

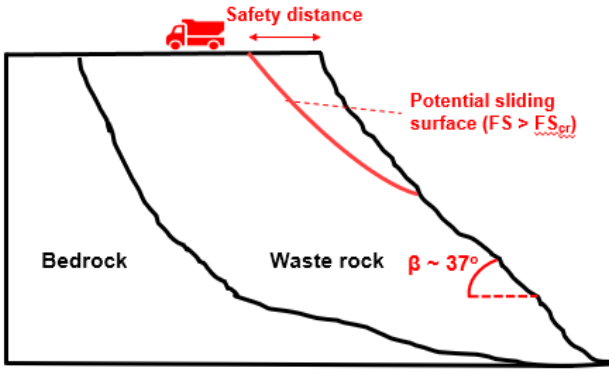

Figure 1. Definition of the safety distance for machinery in end/push-dumping construction for the deposition of waste rock.

The main objective of this article is to analyze the geotechnical behavior and physical stability of high WRPs built by end/push-dumping method in an open-pit mine with backfilling operation, and to estimate the safety distance. Relatively large-scale shearing tests on waste rock are presented, followed by constitutive modeling calibration and finite element modeling (FEM) of WRPs using the software Plaxis (Plaxis, 2021) and the strength reduction technique (Sukkarak et al., 2021). Different pile geometries are modelled, varying the position of the machinery on the top surface of the pile to identify a reliable safety distance. Simulation results are compared with FS values obtained through the limit equilibrium method (LEM) using the software Slope/W (GeoSlope Inc).

The analyses provide valuable insights for safer WRP designs, but it is important to point out that there are aspects and uncertainties that have not been considered here to simplify this complex problem, such as material heterogeneity within the pile (segregation, stratification, different lithologies coming from the mine, etc.), dynamic response, 3D effects, and scatter of WR mechanical parameters, among others.

2 GEOTECHNICAL CHARACTERIZATION OF THE WR MATERIAL

The tested WR material, sampled from a hard rock open-pit mine, is composed by a mixture of different lithologies in the blasted rock (see Figure 2b). Relative density D_r (specific gravity G_s) of the WR material is 2.7. The grain size distribution (Figure 3) of the tested specimens is characterized by a maximum particle size $d_{max} = 50$ mm, no fines, and a uniformity coefficient of $Cu = 7$.

Triaxial compression tests on dry material were carried-out on specimens of $D = 300$ mm (diameter) and $H = 600$ mm (height), under consolidated drained conditions. The size meets the standard ASTM7181-20 aspect ratio, i.e., $D/d_{max} \geq 6$. The specimens were prepared through 10 uncompacted layers of homogeneous material, resulting in an average dry unit weight of 15.7 kN/m^3 (initial void ratio $e = 0.68$); this is deemed to represent loose WR properties following the push-dumping method. Tests were performed at four levels of confining pressures (0.1, 0.2, 0.3, and 0.5 MPa), up to a 15% maximum applied axial strain with the triaxial testing apparatus (see Figure 2a).

Figure 4 presents the main results of the triaxial tests (where $p = (\sigma_1 + 2\sigma_3)/3$ and $q = \sigma_1 - \sigma_3$; effective stresses for dry material). It can be observed that, as expected for loose specimens, the material is highly contractive. An internal friction angle can be computed for the maximum strength measured during each test, assuming a Mohr-Coulomb linear criterion without cohesion in shear/normal stress plane. As shown in Figure 5, the internal friction angle controlling the shear strength of the tested WR material is within the range of values previously reported for rockfills and mine WR (Leps, 1970; Deiminiat et al., 2020; Ovalle et al., 2020).

(a) (b)

Figure 2. (a) Triaxial compression testing device available at Polytechnique Montreal (b) 300/600 mm WR specimen tested.

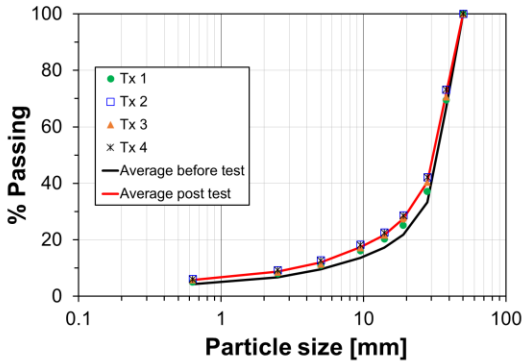

Figure 3. Initial and final particle size distributions of the tested specimens.

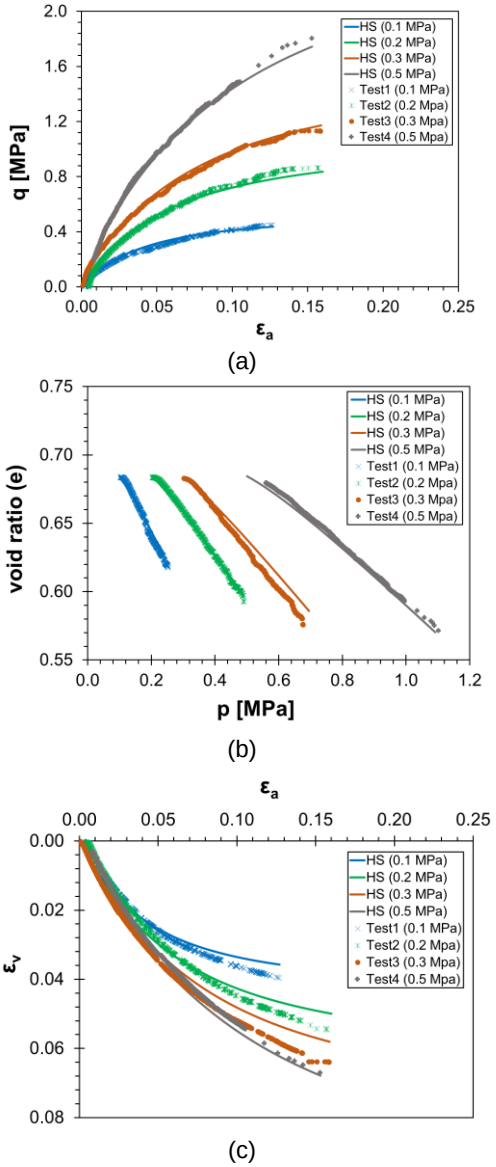

Figure 4. Stress-strain triaxial test results and HS model simulations with calibrated parameters.

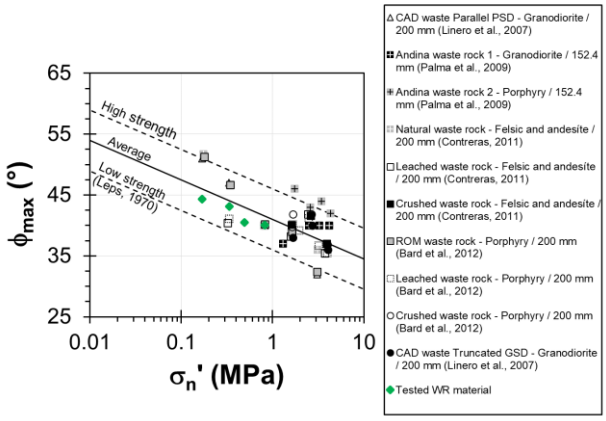

Figure 5. Internal friction angle vs normal stress (modified from Ovalle et al., 2020).

3 HS CONSTITUTIVE MODEL FORMULATION AND CALIBRATION

The Hardening Soil (HS) model has been widely used to represent rockfill material due to its representative features, including double yield surfaces (Schanz et al., 1999; Surarak et al., 2012). The model is based on the following hyperbolic equation proposed by Duncan and Chang (1970):

$$q = \frac{\varepsilon_1}{\frac{1}{E_i} + \frac{\varepsilon_1}{q_a}} \quad [1]$$

where E_i is the initial tangent modulus, q_a as asymptotic deviatoric shear stress at large strain, which can be defined through the failure ratio R_f and peak deviatoric stress q_f ($R_f = q_f/q_a$). As shown in Figure 6, HS model combines two types of yielding surfaces for shear strain hardening and volumetric (cap) strain hardening (Schanz et al., 1999). Flow rules are non-associated for shear and associated for volumetric strain.

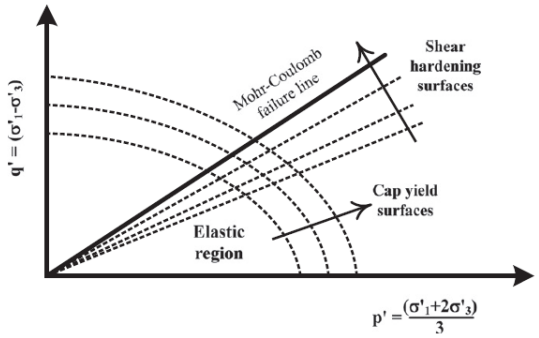

Figure 6. Yield surfaces for the shear strain hardening and volumetric strain (cap) hardening used with the HS model (Surarak et al., 2012).

The stress-strain behavior given by the HS model at primary loading is highly nonlinear and the stress-dependent secant modulus E_{50} (stiffness modulus at 50% mobilization of q_f) is given by:

$$E_{50} = E_{50}^{ref}\left(\frac{c\,cos\phi - \sigma_3 sin\phi}{c\,cos\phi + p^{ref} sin\phi}\right)^m \quad [2]$$

Where c and ϕ are the cohesion and internal friction angle, respectively. All these parameters are related to effective stresses. E_{50}^{ref} is the reference stiffness modulus corresponding to the reference effective stress p^{ref}, and m is a material constant. The stiffness for an unloading-reloading stress path (E_{ur}) and the oedometric stiffness (E_{oed}) are stress-dependent as well, and they are defined using Eq. 2 by replacing E_{50}^{ref} by E_{ur}^{ref} and E_{oed}^{ref}, respectively.

The shear yield function f with non-associated flow rule is given by:

$$f = \frac{1}{E_{50}}\left(\frac{q}{1-\frac{q}{q_a}}\right) - \frac{2q}{E_{ur}} - \gamma^p \quad [3]$$

where the plastic shear strain is defined as $\gamma^p \approx -2\varepsilon_1^p$. The volumetric compression hardening law with associated flow rule, which closes the elastic region in the direction of the mean pressure p (Brinkgreve et al., 2006), is defined as:

$$f^c = \frac{q^2}{\alpha^2} + p^2 - p_p^2 \quad [4]$$

where α as an auxiliary constant (related to the normally consolidated coefficient of lateral earth pressure K_0^{nc}) and p_p is the pre-consolidation effective stress. The hardening law that connects the stress increment $\dot{p}_p$ and the volumetric cap strain rate $\dot{\varepsilon}_c^p$ is given by:

$$\dot{\varepsilon}_c^p = \frac{H}{m+1}\left(\frac{p_p}{p^{ref}}\right)^{m+1} \quad [5]$$

where H is an auxiliary cap parameter (related to K_0^{nc}, E_{ur}^{ref} and E_{oed}^{ref}). The shape of the cap yielding surface in the $p-q$ plane is an ellipse of size given by p_p and H.

For model calibration, strength parameters ϕ, c and R_f were defined to fit the stress ratio q/p at failure, as shown in Figure 8; a very low value of $c = 1$ kPa was used to avoid numerical instabilities related to shallow zones with very low stress in the FEM model. The values of E_{50} were calculated from the stress-strain curve ($q-\varepsilon_1$) presented in Figure 4. The results of E_{50} for each test are then used to evaluate m, E_{50}^{ref} and p_{ref}, fitted to E_{50} vs σ_3. Figure 7 indicates that, the tested material gives results within a similar range of E_{50} for σ_3 less than 1 MPa, when compared to the data reported by Ovalle et al. (2020) on WRs.

In the absence of oedometric tests, the values of E_{oed}^{ref} and E_{ur}^{ref} were approximated using the result of the isotropic compression phase of the drained triaxial compression test.

The above-mentioned calibrated parameters of the HS model were introduced in Plaxis calibration tool to numerically obtain the remaining HS model parameters. The calibration tool uses an optimization algorithm which searches for parameter values within a given range to find the closest curves that fit best the test results (Plaxis, 2021). The failure ratio R_f value is assumed to be 0.9 in all the simulations, which is considered a suitable default setting for rockfill materials (Schanz et al., 1999; Soroush and Aghaei Araei, 2006; Sukkarak et al., 2021). Several sets of calibrated parameters were assessed for a range of shear strength of the tested WR material. The selected parameters are listed in

Table 1, and the results of the tests simulations are shown in Figure 4. It can be observed that the HS model can accurately capture the stress/strain response and evolution of the volumetric strain over the range of stresses applied during the tests. These results confirm that the HS constitutive model is suitable for coarse grained material, as previously reported for rockfills (Soroush and Aghaei Araei, 2006; Xu and Song, 2009; Sukkarak et al., 2021).

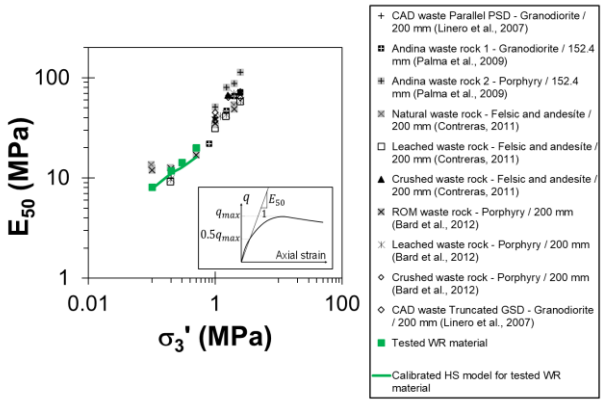

Figure 7. Comparison of E_{50} vs σ_3 for different WR and Rockfill materials (modified from Ovalle et al., 2020).

4 NUMERICAL SIMULATIONS

A 2D base case model of a WRP was defined for backfill disposal in an open-pit, 260 m deep and 600 m long (see Figure 9). As shown in Figure 1, dumping is carried-out from the top of the WR surface, and the material is cumulated over a slope with an average angle β close to 37°, corresponding to its angle of repose.

Several scenarios were considered. After the base case scenario was modeled, different pile heights were simulated with the same $\beta = 37°$. At the next stage, the addition of machinery loads working close to the edge of the slope was considered as static linear distributed loads. The location of the loads was considered at different distances from the edge of the slope in order to estimate a safety distance that could be considered for drivers and operators. The results of all different scenarios for FS were then compared with stress-strain analyses and two different methods of slope stability analysis (LEM in Slope/W of Geo-Studio and strength reduction with FEM in Plaxis).

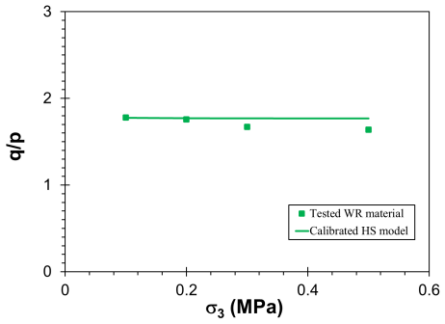

(a)

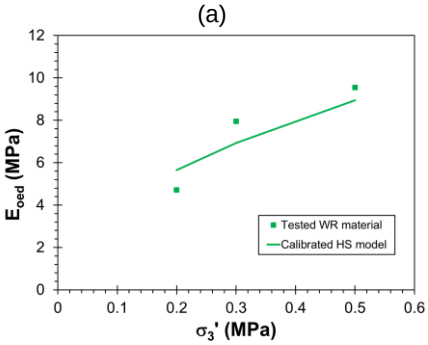

(b)

Figure 8. HS Calibration (a) Stress ratio (q/p) vs σ_3 for tested WR material. (b) Oedometric stiffness vs σ_3.

Table 1. Optimal values of HS calibration for WR material.

Parameter	Unit	Value
E_{50}^{ref}	[MPa]	7.8
E_{oed}^{ref}	[MPa]	4.5
E_{ur}^{ref}	[MPa]	53.1
m	[-]	0.50
p_{ref}	[MPa]	0.1
c	[MPa]	0.001
ϕ	[°]	45
K_0^{nc}	[-]	0.29
R_f	[-]	0.9
ν	[-]	0.2

4.1 LEM simulations

Slope/W is a LEM code, part of the GeoStudio suite (GeoSlope International Ltd, 2017). A user-defined model can be used for the shear strength failure envelope. The defined model used for the tested WR material is a (slightly) non-linear shear strength (τ) vs normal stress (σ_n) curve with two material constants a and b (Charles and Watts, 1980; Hawley and Cunning, 2017):

$$\tau = a{\sigma_n}^b \quad [6]$$

For the tested WR material, calibrated values of a and b are 1.57 and 0.89, respectively. The curve inputted into Slope/W calibrated for tested WR material is shown in Figure 10. In addition, an infinitely rigid material model was assigned for the bedrock under the WRP.

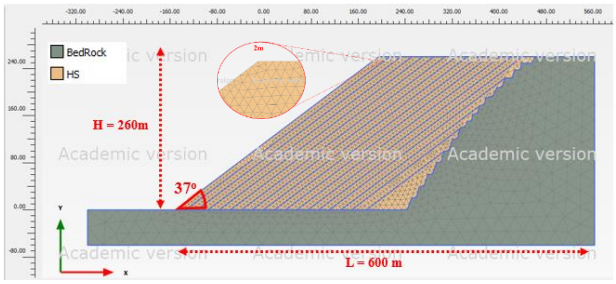

Figure 9. Base case geometry, meshing, and 18 construction stages in the Plaxis model.

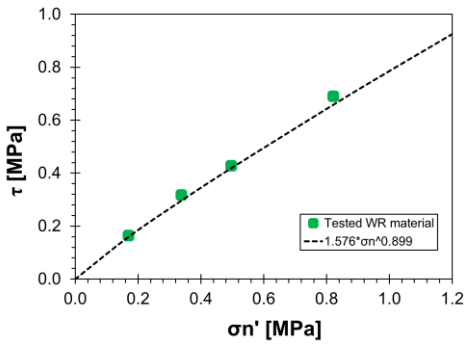

Figure 10. Shear stress τ vs σ_n for tested WR (slightly non-linear relationship with test results).

The commonly used Morgenstern-Price method was applied for slope stability analyses. The results from Slope/W analysis for the base case are presented in Figure 11, while other results for modeled piles with different heights of 200, 150, 100, and 50 m are included in Figure 13. The results of the calculations show that the most critical slip surface (in white in Figure 11) is related to the minimum $FS = 1.21$, while there is a wide range (red zone) that has a variation of $+/-$ 0.1 from the critical FS. Therefore, it is not clear if the whole red zone (around 80 m) should be considered as safety distance, or simply the critical surface.

Figure 13 shows that the FS decreases with increasing the height of the pile, from $FS = 1.4$ for 50 m height, to $FS = 1.2$ for 260 m height.

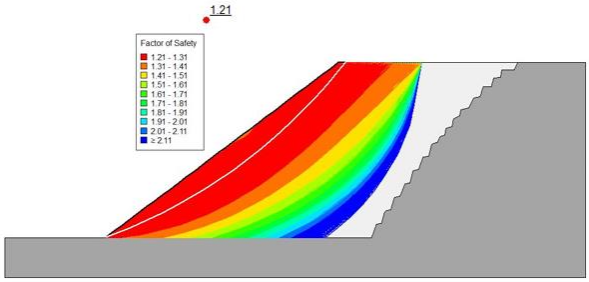

Figure 11. Results from the base case (260 m WRP) analysis in Slope/W; the isocontours show zones with different FS, with the critical slip surface ($FS = 1.21$).

Improved estimate for the safety distance could be obtained using FEM simulations after calibration of the stress/stress behavior of the WR material, as shown in the next section.

4.1.1 FEM simulations

HS model calibrated parameters presented in Table 1 were used for the WR material. The bedrock foundation was modeled as hard strong material defined by an elastic model with high value of $E = 15$ MPa, and $v = 0.2$. As boundary conditions, vertical and horizontal displacements were blocked at the base and at the sides of the bedrock layer for all the analyses. A refined triangular mesh with a minimum side length of 2 m was generated for the model; this was deemed appropriate to avoid the effect of mesh size. A total of 18 inclined layers of WR were defined to simulate the construction stages (see Figure 9) and recreate the stress history during construction.

To conduct slope stability analyses and compute the FS, Plaxis includes the strength reduction (RS) method (Plaxis, 2021). The value FS of a slope is then defined as the factor by which the shear strength parameters (c and ϕ) must be reduced to bring the slope to failure (e.g., Griffiths and Lane,1999). The corresponding definition of FS in Plaxis for cohesionless WR (based on ϕ reduction) becomes:

$$FS = \frac{tan\phi}{(tan\phi)_f} \qquad [7]$$

where $(tan\phi)_f$ represents the reduced friction coefficient. The software gradually reduces $(tan\phi)$ until numerical non-convergence (Plaxis, 2021).

The results of Plaxis simulations for the base case are presented below. The maximum deviatoric stress q (near the pile base) after 18 construction stages is around 3 MPa (see Figure 12a). The RS method applied with Plaxis leads to results in Figure 12b (in terms of incremental shear strain), which shows the location of the most critical slip surface obtained, with $FS = 1.16$.

Different pile heights of 200, 150, 100, and 50 m were also simulated in Plaxis. The results are compared in Figure 13 in terms of FS, showing slightly lower values for FEM simulations with the HS constitutive model compared to those from LEM analyses (with an average FS decrease of about 0.05). For reference, the infinite slope stability FS value of the WRP (for cohesionless soils: $tan\phi/tan\beta$ with $\phi = 45^o$ and $\beta = 37^o$) is 1.33, which is higher than both FS values from FEM and LEM analyses.

Safety distance from the edge

Aiming to estimate a safety distance for machinery to work securely, two static linear distributed loads of 130 kN/m for the dozer, with a 6 m length, and 290 kN/m for the truck, with a 13 m length, were added on the top surface of the WRP. These loads were based on the typical weight and size of the machinery (truck and dozer) working on top surface of WRP (total weight/length of the machine). The distance between the two machines was taken as 12 m, which is the typical range that the dozer usually pushes the WR material. The FEM result of one of the modeled cases with machinery load (located 14 m from the edge of the pile) is presented in Figure 14 in terms of total displacement of the completed pile. The simulation results indicate that the addition (and position) of the machinery has a relatively small but non-negligible effect on total displacement (around 5% higher values compared to the base case); the impact on FS is also small, as shown below.

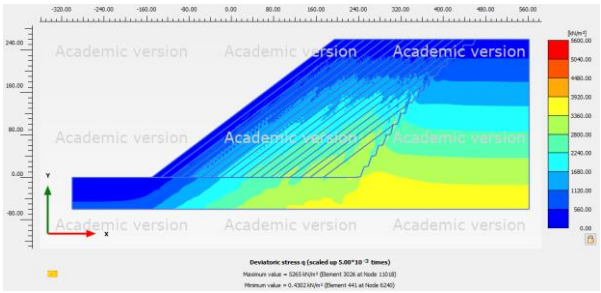

(a)

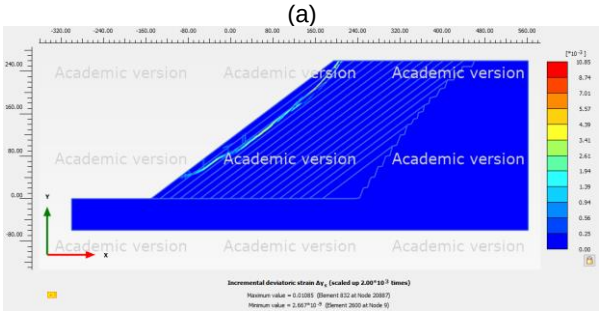

(b)

Figure 12. Plaxis simulation results: (a) total deviatoric stress q distribution after the 18th construction stage, (b) most critical slip surface obtained for the base case after a slope stability analysis with the RS method ($FS = 1.16$).

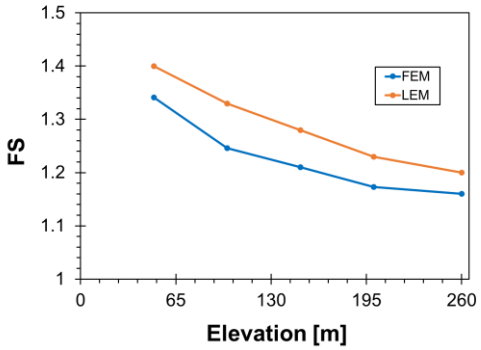

Figure 13. Variation of FS vs elevation of the modeled WRPs, obtained with the two methods of analysis.

Additional simulations were performed to consider different locations of the machinery from the edge of the slope. The simulations were repeated for the 150 m high WRP and the results are compared in Figure 15. At each simulation, the distance of the most critical slip surface from the edge of the pile has been taken as the corresponding safety distance. Figure 15a indicates that the value of FS slightly decreases when machinery approaches the edge of the pile; the values become very similar to the initial value (without machinery) at a distance of about 20 to 25 m from the edge. Figure 15b shows that the safety distance seems to depend on the machinery location up to a certain point, beyond which it appears to remain constant, regardless of the machinery location.

Simulations of the 150 m WRP show shallower slip failure and lower safety distance compared to the base case.

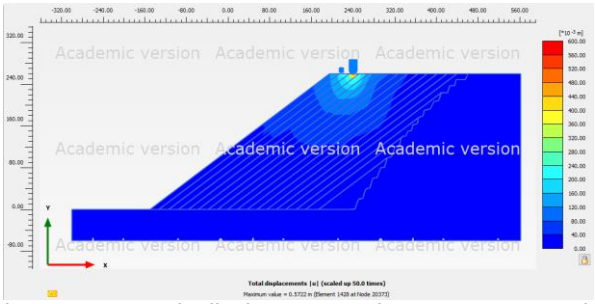

Figure 14. Total displacement of a 260 WRP with machinery load at 14 m from the edge of the WRP.

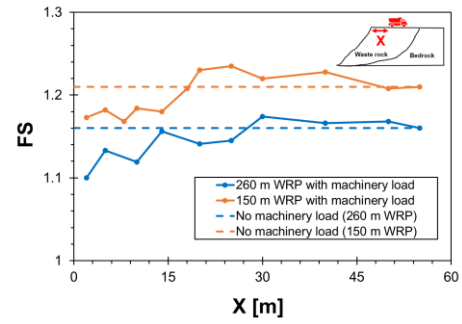

(a)

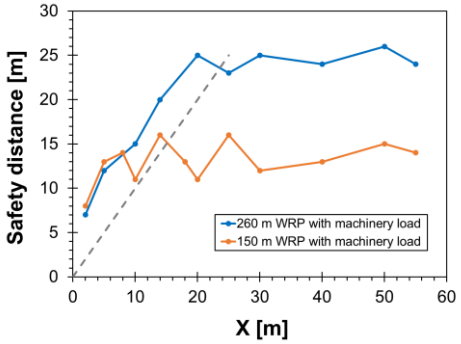

(b)

Figure 15. Effect of machinery's load location on variation of (a) FS and (b) safety distance (the distance between critical slip surface and edge of the WRP).

5 CONCLUSION

Slope stability of WRPs built by the end/push dumping method is sensitive to many factors, such as the height of the pile, the material properties, the load of the machinery operating on the top surface of the pile, among others. Despite the value and simplicity of commonly used LEM for the analysis of WRP stability, these methods do not consider the stress-strain behavior of the slope. FEM simulations with a comprehensive constitutive model provide a more realistic stress-strain behavior of WRPs, leading to a more representative stability analysis for different conditions.

The parameters of the Hardening Soil constitutive model were calibrated using triaxial test results on WR from a hard rock mine. The calibrated model was employed in a FEM code and the results of stability analysis conducted with the strength reduction method were compared to the results of a LEM model. The effect of machinery load at various distances from the pile's edge with different pile heights was considered. The results were used to estimate a safety distance for machinery to work securely on top of the WRP. Conclusions of this study can be summarized below:

- FS of WRPs tends to decrease with the height of the pile.
- LEM slightly overestimates FS by an average of 0.05, in comparison to FEM calculations.
- The results of LEM simulations do not give a precise value of the safety distance, as a there is a wide extension zone on top of the pile that has an almost constant FS $(+/-\ 0.1)$.
- FEM modeling provides a more specific location of the sliding surface, allowing a more specific estimate of the safety distance depending on the machinery location on top of the pile.
- The FS slightly decreases when machinery approaches the edge of the slope. For a 260 m height WRP, the FS becomes similar to the case without machinery at a distance of about 25 m from the edge. This distance could however be increased significantly for higher values of FS, sometimes recommended for waste rock piles (e.g., Maknoon and Aubertin 2021).
- The safety distance is directly dependent on the machinery location up to a certain location; for distances higher than about 25 m it remains constant, regardless of the machinery location.

The main results presented here are representative of a specific type of WRPs built in an open-pit mine by the end/push dumping method. Despite the specific aspects presented in this paper, there are still many uncertainties that should be considered in future studies, such as sensitivity of the safety distance to small variations of the FS, more complex pile geometries (benches, layering, etc.), material heterogeneity within the pile (segregation, stratification, different lithologies, etc.), construction stages, dynamic response, 3D effects, scatter of WR mechanical parameters after comprehensive testing, among others.

6 REFERENCES

ASTM D7181-20 (2020). Standard test method for consolidated drained triaxial compression test for soils, ASTM International, West Conshohocken, PA. doi:10.1520/D7181-20.

Aubertin, M., Bussière, B., & Bernier, L. (2002). Environnement et gestion des rejets miniers. Manual on CD-rom. Presses internationales Polytechnique..

Aubertin, M., Maknoon, M., Ovalle, C. (2021): Waste rock pile design considerations to promote geotechnical and geochemical stability. Canadian Geotechnique – The CGS Magazine: Fall 2021, 2(3), pp. 44-47

Bar, N., Semi, J., Koek, M., Owusu-Bempah, G., Day, A., Nicoll, S., & Bu, J. (2020). Practical waste rock dump and stockpile management in high rainfall and seismic regions of papua

new guinea. 2020 international symposium on slope stability in open pit mining and civil engineering, Australian Centre for Geomechanics, Perth, pp. 117-128.

Brinkgreve, R. B., Kumarswamy, S., & Swolfs, W. M. (2006). Plaxis material models manual. TheNetherlands.

Charles, J. A., & Watts, K. S. (1980). The influence of confining pressure on the shear strength of compacted rockfill. Geotechnique, 30(4), 353-367.

Dawson, R.F., Morgenstern, N.R., & Stokes, A.W. (1999). Liquefaction flowslides in Rocky Mountains coal mine waste dumps: Canadian Geotechnical Journal, 35(2), 328-343.

Deiminiat, A., Li, L., Zeng, F., Pabst, T., Chiasson, P., & Chapuis, R. (2020). Determination of the shear strength of rockfill from small-scale laboratory shear tests: A critical review. Advances in Civil Engineering, 2020.

Duncan, J.M., & Chang, C.Y. (1970). Nonlinear analysis of stress and strain in soils. J. of the soil mechanics and foundations division, 96(5), 1629-1653.

GeoSlope International Ltd. (2017). Stability Modeling with GeoStudio.

Griffiths, D. V., & Lane, P. A. (1999). Slope stability analysis by finite elements. Geotechnique, 49(3), 387-403.

Hawley, M., & Cunning, J. (2017). Guidelines For mine waste dump and stockpile design csiro publishing, 2017.

Leps, T. (1970). Review of Shearing Strength of Rockfill. Journal of the Soil Mechanics and Foundations Division, 1970, Vol. 96, Issue 4, Pg. 1159-1170

Maknoon, M. & Aubertin, M. (2021). On the Use of Bench Construction to Improve the Stability of Unsaturated Waste Rock Piles. Geotechnical and Geological Engineering, 39(2): 1425-1449.

Ouellet, S., Chapuis, S., Ovalle, C. (2021). Le projet de co-déposition dans la fosse Canadian Malartic. Symposium Rouyn-Noranda 2021 sur l'environnement et les mines. Université du Québec en Abitibi-Témiscamingue (UQAT).

Ovalle, C., Linero, S., Dano, C., Bard, E., Hicher, P.-Y., Osses, R. (2020): Data compilation from large drained compression triaxial tests on coarse crushable rockfill materials. Journal of Geotechnical and Geoenvironmental Engineering 146(9): 06020013

Plaxis, B. V. (2021). PLAXIS 2D CE V22.00. Reference Manual. The Netherlands.

Schanz, T., Vermeer, P. A., & Bonnier, P. G. (1999). The hardening soil model: formulation and verification. In Beyond 2000 in computational geotechnics-10 years of Plaxis, Balkema, Rotterdam, pp. 281–296.

Soroush, A., & Aghaei Araei, A. (2006). Analysis of behaviour of a high rockfill dam. Proceedings of the Institution of Civil Engineers-Geotechnical Engineering, 159(1), 49-59.

Sukkarak, R., Likitlersuang, S., Jongpradist, P., & Jamsawang, P. (2021). Strength and stiffness parameters for hardening soil model of rockfill materials. Soils and Foundations, 61(6), 1597-1614.

Surarak, C., Likitlersuang, S., Wanatowski, D., Balasubramaniam, A., Oh, E., & Guan, H. (2012). Stiffness and strength parameters for hardening soil model of soft and stiff Bangkok clays. Soils and foundations, 52(4), 682-697.

Valenzuela, L., Bard, E., Campana, J. & Anabalon, M. (2008). High Waste Rock Dumps - Challenges and Developments. Rock Dumps — A. Fourie (ed). Australian Centre for Geomechanics, Perth

Xu, M., & Song, E. (2009). Numerical simulation of the shear behavior of rockfills. Computers and Geotechnics, 36(8), 1259-1264.